Wind Speed Estimation From CYGNSS Using Artificial Neural Networks

Jennifer Reynolds, Maria Paola Clarizia, *Senior Member, IEEE*, and Emanuele Santi, *Member, IEEE*

***Abstract*—In this article, a retrieval algorithm based on the use of an artificial neural network (ANN) is proposed for wind speed estimations from cyclone global navigation satellite system (CYGNSS). The delay/Doppler map average and the leading edge slope observables, derived from CYGNSS delay/Doppler maps, are used as inputs to the network, along with geographical, geometry, and hardware antenna information. The derivation of the optimal number of hidden layers and neurons is obtained using statistical metrics of agreement between the CYGNSS data and the wind matchups obtained from modelled winds output by the wavewatch 3 (WW3) model. A cumulative distribution function (CDF) matching step is applied to the network outputs, to impose that the CDF of the retrievals matches that of the matchups. The resulting wind speeds are unbiased with respect to WW3 modeled winds, and deliver a global root mean square (RMS) difference (RMSD) of 1.51 m/s, over a dynamic range of wind speeds up to 32 m/s. The obtained RMSD is the lowest among those seen in literature for wind speed retrievals from CYGNSS. A comparison is carried out between the winds retrieved from the ANN approach and those derived using the fully developed sea approach, which represent the CYGNSS baseline wind product. The comparison highlights that the ANN approach outperforms the baseline approach for both low and high wind speeds and removes most of the geographical biases between baseline winds and WW3 winds seen in monthly maps of wind speeds. The ANN approach could well be applied to the entire CYGNSS dataset to generate an enhanced wind speed product.**

***Index Terms*—Artificial neural network (ANN), cyclone global navigation satellite system (CYGNSS), global navigation satellite system-reflectometry (GNSS-R), wind speed.**

I. Introduction

GLOBAL navigation satellite system-reflectometry (GNSS-R) is a passive remote sensing technique that uses global navigation satellite signals reflected off of the Earth's surface to gain information about the characteristics of those surfaces. By using signals that are already in space, GNSS-R is a cost-effective way of collecting valuable data for the derivation of geophysical parameter, requiring only receivers to be built for specific missions. The most successful example of GNSS-R mission is the cyclone global navigation satellite system (CYGNSS) mission [1], designed primarily for the purpose of monitoring tropical cyclones [2]– [5], but collecting data over all of the oceans and providing global retrievals of wind speeds [6]–[8]. These retrievals are achieved using the so-called baseline approach that implements the minimum variance combination of wind estimates from two observables, derived from CYGNSS delay/Doppler maps, and known as delay/Doppler map average (DDMA) and leading edge slope (LES) [6] [8]. The wind speed estimates derived from each of these observables are obtained via the development of geophysical model functions (GMFs), which consist of 2-D lookup tables of retrieved wind speed, function of the observable and the incidence angle [8]. The baseline winds provide good quality global wind estimates which have been shown to meet the mission requirements [9], but suffer from significant retrieval biases, especially at high wind speeds [1], [10]. This study demonstrates that a significant improvement in the wind speed estimation can be globally achieved through the use of an Artificial Neural Network (ANN) approach, providing global estimates of wind speeds which are better than the baseline ones over the full dynamic range of wind speeds.

ANN are aimed at providing a minimum variance solution to the given problem. If appropriately trained, ANN are able to reproduce almost any relationship between inputs and outputs [11], [12]. ANNs were successfully employed in solving a wide variety of remote sensing problems [13]–[15], since they offer an easy but effective possibility of combining input data from different sources into the same retrieval algorithm [16].

In particular, ANNs have been widely applied in the context of wind speed retrieval from scatterometers [17], [18], and more recently they have been used within the GNSS-R field. ANNs in combination with a particle filter and particle swarm optimization have been exploited for ocean wind speed estimations in coastal regions, using Beidou satellite data, and in the days surrounding Typhoon Utor [19], [20]. Other Machine Learning (ML) approaches have also been proposed for the retrieval of wind speed using GNSS-R data from both TechDemoSat-1 [21] and CYGNSS [22]. ANNs and convolutional neural networks have also been used for purposes other than the wind speed, such as Sea Ice Detection and Sea Ice Concentrations estimation using GNSS-R Delay Doppler Maps [23], [24]. More generally, in the field of remote sensing ANNs have been used widely, for instance for forecasting SWH [25], estimating precipitation from remote sensing information [26] and sea surface temperature forecasting [27] among other applications. In this article, an ANN approach is applied to CYGNSS data for ocean wind speed

Manuscript received October 10, 2019; revised December 20, 2019; accepted January 6, 2020. Date of publication February 5, 2020; date of current version February 20, 2020. This work was supported in part by the University of Michigan and Deimos Space UK Limited, under the Contract SUBK00009666 and in part by NASA under Contract NNL13AQ00C. *(Corresponding author: Jennifer Reynolds.)*

Jennifer Reynolds and Maria Paola Clarizia are with Deimos Space UK Ltd., Harwell OX11 0QR, U.K. (e-mail: jennifer.reynolds@deimos-space.com; maria-paola.clarizia@deimos-space.com).

Emanuele Santi is with Istituto di Fisica Applicata "Nello Carrara,", Consiglio Nazionale delle Ricerche, 00185 Rome, Italy (e-mail: e.santi@ifac.cnr.it).

Digital Object Identifier 10.1109/JSTARS.2020.2968156

estimation. The approach proposed in this article is simple and computationally effective, and at the same time provides wind speed retrievals with improved performance compared to all the approaches existing in literature for wind speed estimation from CYGNSS data. In particular, the ANN algorithm proposed here yields unbiased wind speed estimates with a global root mean square difference (RMSD) of 1.51 m/s, over a wind speed range from 0 m/s to 32 m/s. The achieved RMSD is lower than the other RMSD values obtained from other wind speed retrieval algorithms for CYGNSS [8], [9], [22], [28], [39]. The approach analyzed in this paper differs in particular quite significantly from that illustrated in [22], where an ANN is also used, but with different input parameters both in number and type, and with a number of layers and neurons of the network unspecified. The network adopted in this study is a feed-forward network whereas the one in [22] uses a backpropagation algorithm to derive the optimal wind speed estimates. The results obtained in this article outperform those illustrated in [22], and are more robust since they are derived using a CYGNSS dataset composed of tens of millions of samples, compared to the 40 000 samples used in [22]. The methodology for wind speed estimation proposed in this study uses an ANN with a number of inputs to learn the complex relationships between the inputs and the output and to produce reliable estimates of the wind speed. The winds estimated from the ANN also undergo a Cumulative Distribution Function (CDF) correction similar to what is conventionally done in scatterometry [29], which contributes to a further improvement of the final results. The obtained wind speed estimates are compared in particular to the wind speed retrievals under Fully Developed Seas (FDS), derived using the CYGNSS baseline algorithm [8]. It is shown that the ANN based estimates exhibit improvements compared to the baseline approach generally everywhere, and reproduce better the high wind speed region. This region tends to be generally problematic for conventional algorithms [1], [8], [10] but could easily benefit from the use of ANNs, provided that a sufficiently high number of high wind occurrences can be included in the training dataset as input to the ANN. The technique here is demonstrated using two months of CYGNSS data, which already represents a large amount of data samples to both test and train the network, that span a large range of wind speed conditions. The rest of this article is organized as follows. Section II describes the datasets used and the filtering applied. Section III explains the implemented ANN configuration and the optimal parameters for the ANN. Section IV illustrates the results globally and statistical analysis; Finally, Section V concludes this article.

II. Data

The data used are CYGNSS Level 2 version 2.1, filtered in order to obtain the best quality data. The criteria used for the filtering are the same as in [28], but are here repeated for convenience:

1) the observables need to have good quality, which is determined by the Quality Control (QC) flag in the data;
2) the observables as well as the wind speed matchups need to be positive;
3) the measurements taken when the star tracker is not tracking due to solar contamination are discarded;
4) the measurements from the GPS Block type II-F satellites are discarded, due to the lack of accurate information on the transmitter antenna gain pattern for this family of GPS satellites;
5) the Range-Corrected Gain (RCG) of the measurements is higher than 3. The definition and description of RCG can be found in [6];

The data spanned the period August 1 to November 30, 2017 and post filtering 72 million samples remained for use in the ANN. Modelled ocean surface wind speeds output from the wavewatch 3 (WW3) model [40] with input wind forcing from the European Centre for Medium-Range Weather Forecast [30] were used as reference matchups. These matchups cover a wind speed range from 0 m/s to 32 m/s.

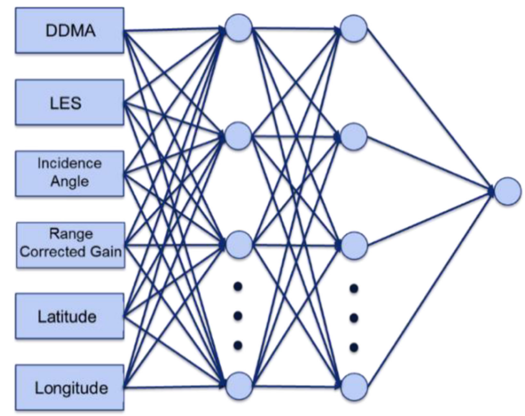

Fig. 1. Simplified visualization of the artificial neural network.

III. Methodology

In this section, we describe the approach used to estimate wind speed, based on the use of Artificial Neural Networks and the subsequent CDF matching correction.

A. ANN Configuration

Artificial neural networks (ANNs) are a relatively simple machine learning tool that allows complicated tasks to be completed quickly, by learning relationships that exist between the input and the output. ANNs consist of at least 3 layers: an input layer, a hidden layer or layers and an output layer as shown in Fig. 1. Each layer contains neurons with each neuron connected to every neuron in the following layer, in this way resembling the structure of a biological neural network [31]. The number of hidden layers used in an ANN is generally between 1-3 and 4 or more are rarely used [32]. The ANNs used for this study are feed forward networks where information is passed from the input layer through the hidden layer(s) and out to the output layer in a forward pass [33]. The training is based on the back propagation learning rule (BPR) [34]: it is a gradient descent algorithm aimed at minimizing the MSE between predicted outputs and target values by adjusting the network parameters

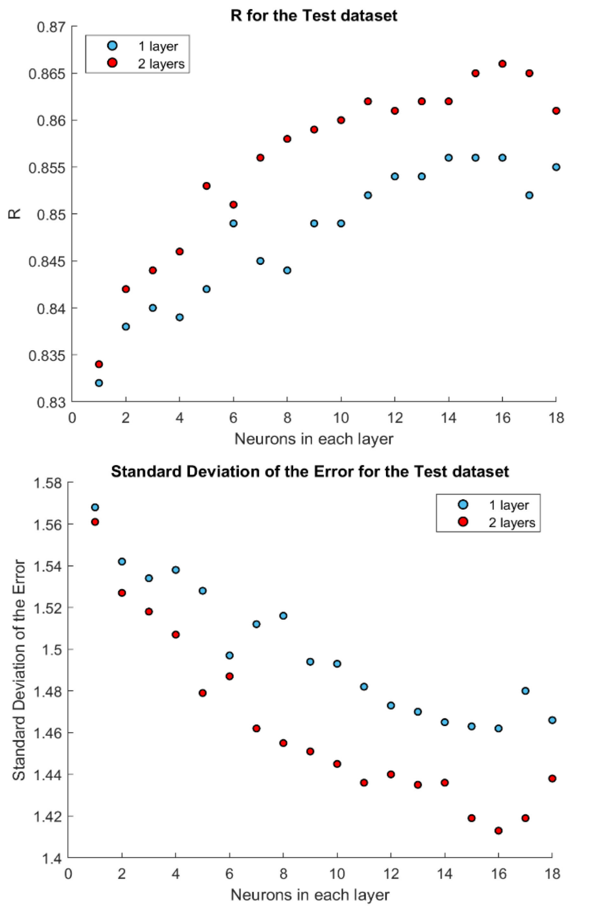

Fig. 2. (Top) Correlation coefficient and (bottom) standard deviation of the Error when varying the number of neurons in each layer and the number of layers.

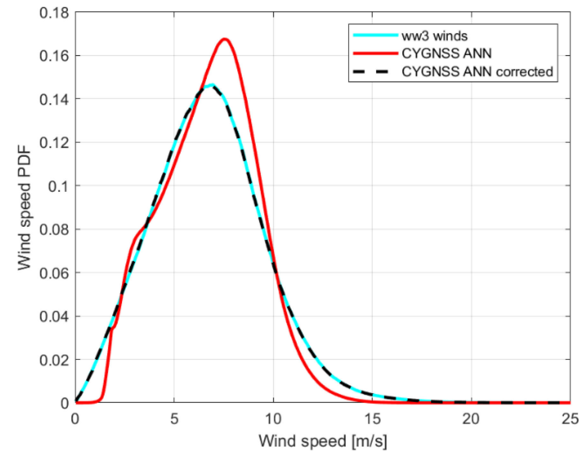

Fig. 3. PDFs of ground truth WW 3 winds (cyan), winds output by ANN (red) and final retrieved winds (dashed black).

TABLE I
BIAS AND RMSD STATISTICS FOR ANN AND FDS FOR ALL WINDS

All U_{10}	ANN Winds	FDS Winds
Bias [m/s]	0.01	-0.01
RMSD [m/s]	1.51	1.77

TABLE II
BIAS AND RMSD STATISTICS FOR WINDS BELOW OR EQUAL TO 12 m/s.

$U_{10} \leq 12$m/s	ANN Winds	FDS Winds
Bias [m/s]	-0.04	-0.08
RMSD [m/s]	1.44	1.71

TABLE III
BIAS AND RMSD STATISTICS FOR WINDS ABOVE 12 m/s.

$U_{10} > 12$ m/s	ANN Winds	FDS Winds
Bias [m/s]	1.62	1.95
RMSD [m/s]	2.80	2.98

(i.e. weights and biases). Overfitting is a common potential problem when using ANNs, which occurs when the network has been trained to accurately predict the output for the training dataset but performs poorly on a new test dataset [35]. In order to avoid overfitting, two separate datasets were used, one for training and one for validation [16], so that any overfitting could be spotted by checking and ensuring that the errors for both were similar. The training dataset is further split randomly into a training set and two test sets, composed of 70%, 15% and 15% of the dataset, respectively. The first subset served for training the ANN by using BPR and the other two subsets served to have two independent tests of the network at each training iteration. Based on the early stopping rule [35], training stops either when the training error has stopped decreasing for a certain number of iterations, in this case after 6 iterations, or when the error on the three datasets starts diverging. The scope was again in avoiding overfitting.

The configuration that was used consists of 2 hidden layers with 16 neurons in each layer with the use of the logistic sigmoid transfer function. Such configuration was chosen as a trade-off between reaching good performances and good correlation between retrieved winds and matchups for the test dataset and computational efficiency, as more hidden layers and/or neurons translates into higher computational expenses [23]. 6 inputs were put into the input layer made up of: DDMA, LES, Incidence Angle, Range Corrected Gain or RCG [6], Latitude and Longitude of the specular point acquisition. A simplified view of the ANN is shown in Fig. 1. Latitude and Longitude were also included as inputs as they provided a slight improvement to the final results. When including latitude and longitude as inputs to the ANN, the correlation coefficient increased by 2.5% and the RMSE decreased by around 7%. This means that the network uses some geographical information about the wind speed range and distribution, but such information is not the dominant source for estimating the winds themselves. The data were randomly split into the two datasets composed of 1/9 and 8/9 of the total dataset, for training and validation, respectively. This ratio was determined as a trade-off between the need to have a training dataset representative enough of the behavior of the overall data and the need to keep the computational time

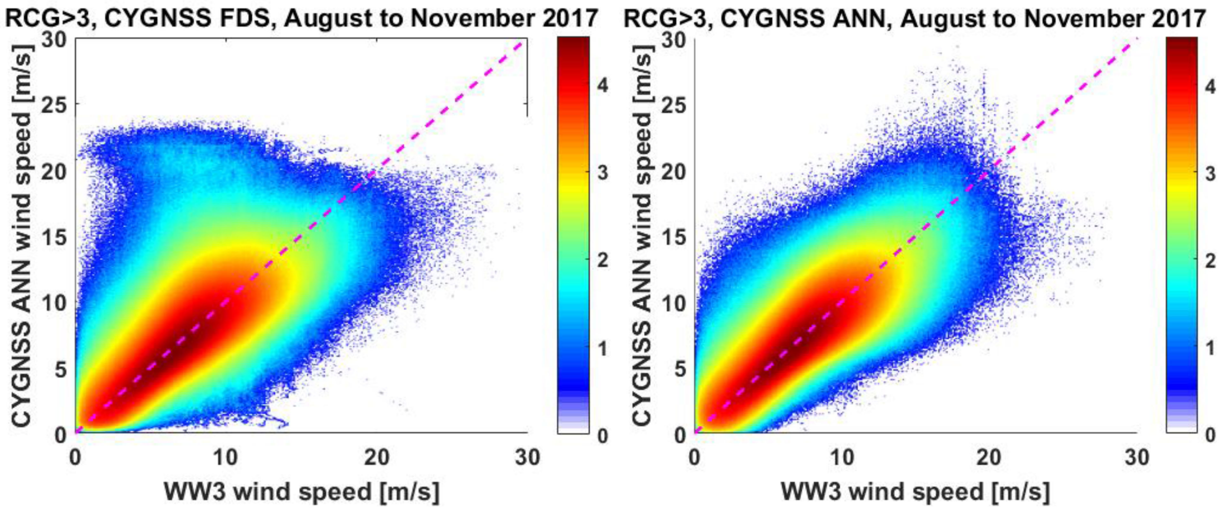

Fig. 4. (Left) Density plot in log-scale of WW3 winds versus CYGNSS FDS winds, for the test dataset. (Right) Density plot in log-scale of WW3 winds versus CYGNSS ANN winds, for the test dataset. A filter of range-corrected gain higher than 3 is applied to the processed data.

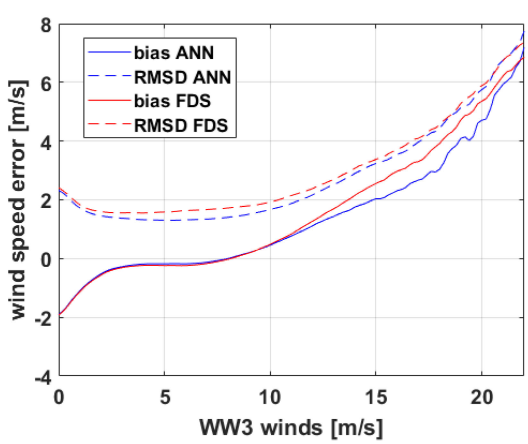

Fig. 5. Bias and RMSD for the FDS winds and the ANN winds.

for the network determination acceptable. The training dataset contained 8 million samples, the validation dataset contained the remaining samples, around 64 million.

B. Choice of Optimal Parameters for ANN

Here we discuss how the final number of neurons and layers was chosen for the ANN. The two metrics chosen to determine such optimal numbers are the correlation coefficient and the standard deviation of the error between retrieved winds and matchups for the test dataset. Fig. 2(a) shows the variability of the correlation coefficient R as a function of number of neurons and hidden layers. It is shown that having two hidden layers always produces a better correlation coefficient compared to one hidden layer only, independent of the number of neurons. The correlation coefficient also clearly increases with the number of neurons in each layer, reaching a peak of 16 neurons after which it starts to decrease for increasing number of neurons.

Fig. 2(b) shows the variability of the standard deviation of the error as a function of number of hidden layers and neurons.

Once again, having two hidden layers produces a lower standard deviation value than having one hidden layer for the same number of neurons. The number of neurons providing the lowest possible standard deviation of the error is 16, consistent with the behavior of the correlation coefficient. Hence a neural network with two hidden layers and 16 neurons in each layer was considered as the optimal configuration for this analysis.

C. CDF Matching

The winds retrieved from the ANN undergo a CDF matching approach, as final step to obtain the final wind estimates. This is a technique commonly adopted for wind speed retrievals in scatterometry [29] recently applied also to GNSS-R [28], [36], and consists of imposing that the CDF of the retrieved winds be equal to the true CDF of winds speeds, where the latter is density function (pdf) of retrieved winds is also obtained from modeled global WW3 winds. The CDF matching approach implies that the probability matched up to that of the true winds. Fig. 3 shows the pdf of the winds output by the ANN in red, and how different it is compared to the true pdf of winds in cyan. The dashed black function represents the pdf of the final retrieved winds after the CDF matching correction, which coincides with the true pdf. The CDF matching step is important as it removes the bias from the final estimates, and it improves the overall agreement between estimates and matchups, even though at the expense of a slight increase of the overall root mean square (RMS) Difference compared to that obtained from the ANN outputs without such correction. In particular, the CDF matching correction improves the low and high wind speed estimates, as the ANN tends to overestimate the low winds and underestimate the high winds. In the sections that follow, the winds obtained

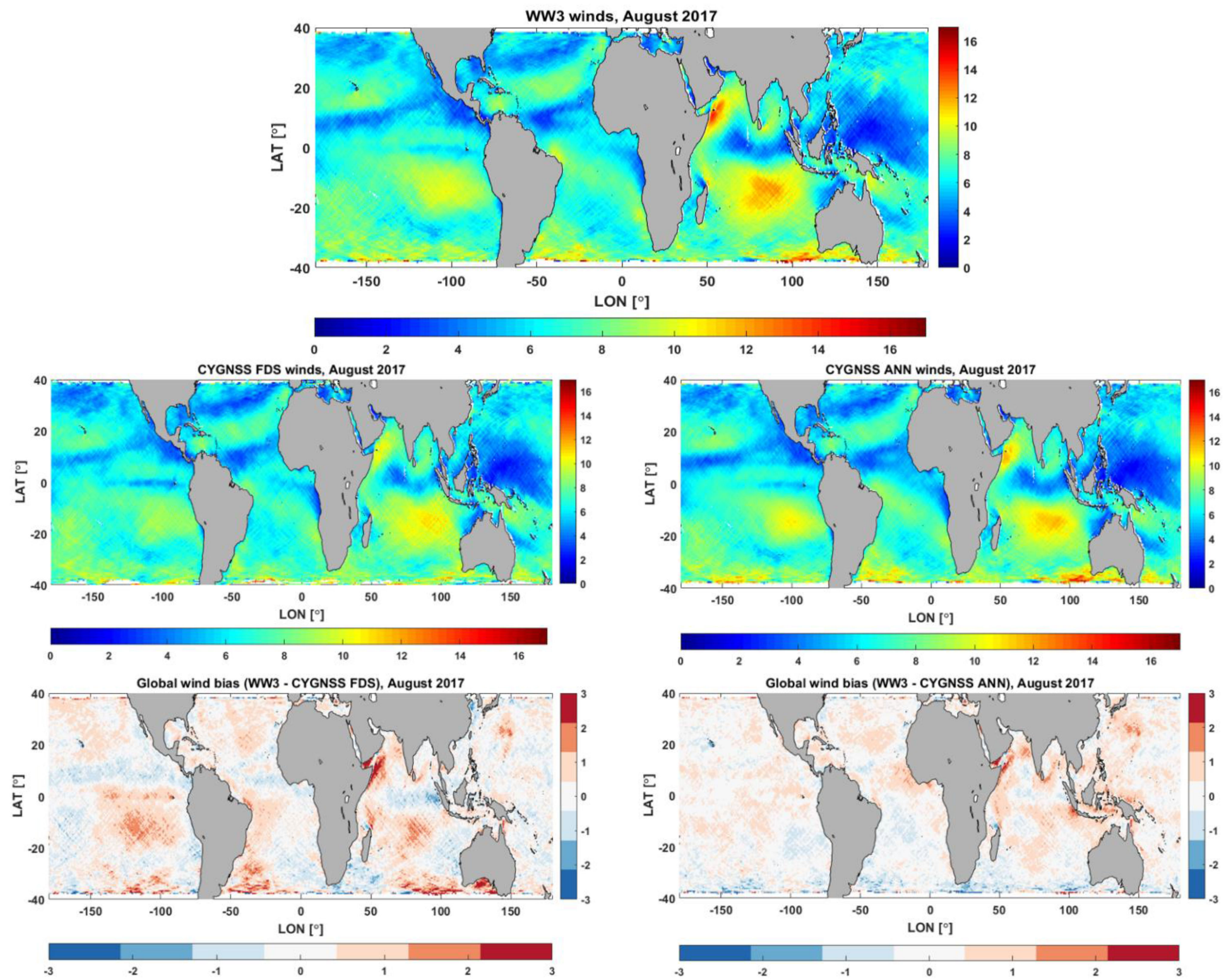

Fig. 6. Illustration of global monthly gridded maps for August 2017. (Top) WW3 winds; (middle left) CYGNSS FDS winds; (Bottom left) Wind bias, computed as WW3 winds minus CYGNSS FDS winds; (middle right) CYGNSS ANN winds; (bottom right) Wind bias, computed as WW3 winds minus CYGNSS ANN winds.

from the combination of ANN and CDF matching step are for brevity called ANN winds.

IV. Results

Here we present the results for the ANN methodology on a global scale. Fig. 4(b) shows a log-density plot of ANN winds versus the WW3 matchups, for the test dataset, and it is compared to the density plot of baseline FDS winds in Fig. 4(a) which represent the official baseline L2 CYGNSS product. The FDS baseline winds were obtained from a GMF trained on winds from the Global Data Assimilation System (GDAS), which are slightly different from WW3 winds. Moreover, they are obtained by implementing a time-averaging step [37] which smooths out the retrievals to improve their accuracy, at the expense of the spatial resolution. The ANN winds are symmetrically centered around the 1:1 line across the whole wind speed regime, and the data spreading around the 1:1 line also appears reduced compared to the FDS winds, as well as those from other algorithms that are an improvement with respect to the baseline case [28]. There is also more agreement in the high wind speed regime (i.e. winds higher than 15 m/s) for the ANN case, and the visible "bump" in the FDS wind plot, where WW3 winds around 7 m/s are mapped into CYGNSS wind speed estimations higher than 15 m/s, disappears in the ANN plot.

Fig. 5 shows global statistics for both the ANN winds and the FDS winds, in the form of bias (mean error) and RMSD, plotted against the reference WW3 wind speed. Both the bias and the RMSD are slightly lower in the ANN case compared to the FDS case, for the full range of wind speeds considered for the analysis, consistent with the findings in Fig. 4. The improvement is small up until winds of $\sim$12 m/s, even though this represents the majority of the population. For winds above 12 m/s, the ANN improvement is stronger, especially for the bias, and increases for increasing wind speed. Table I illustrates the overall performances of the ANN and FDS algorithm for all winds, while Tables II and III show the performances respectively for winds below 12 m/s and above 12 m/s.

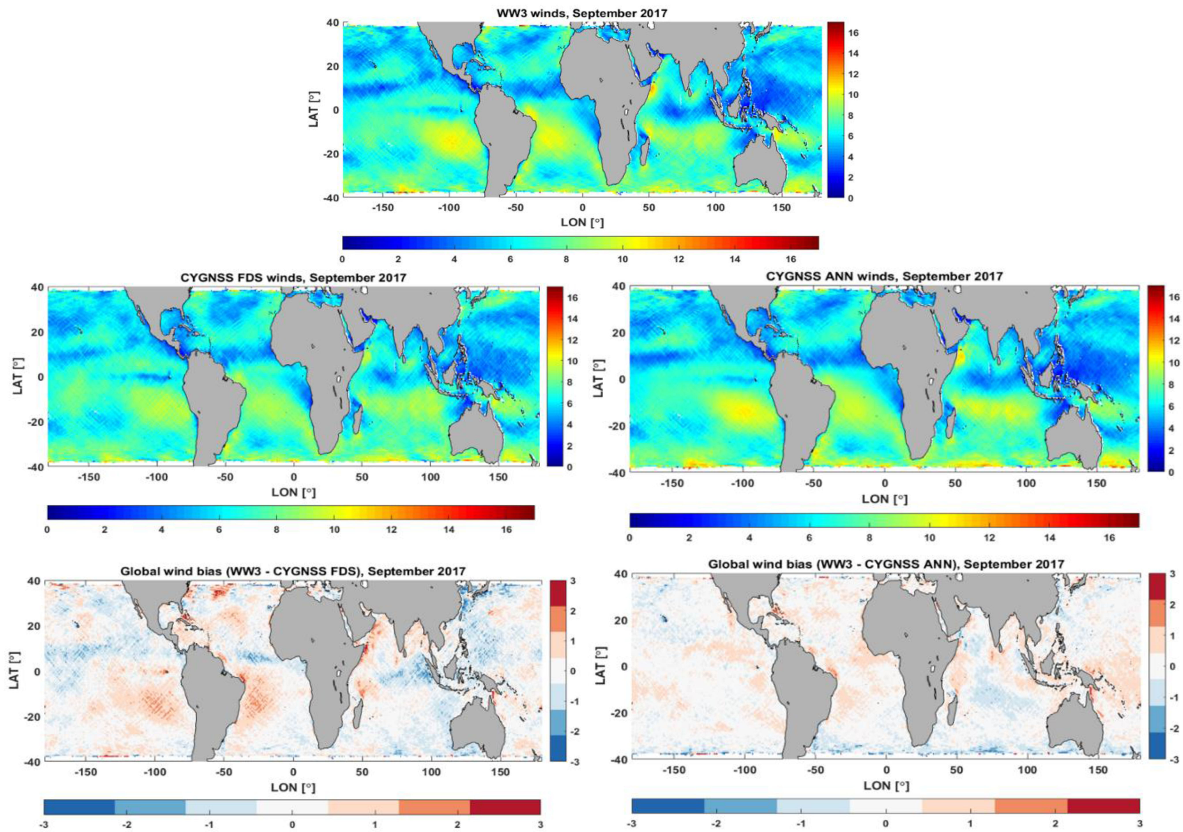

Fig. 7. Same as Fig. 6 but for September 2017.

TABLE IV
BIAS, RMSD, AND CORRELATION COEFFICIENT COMPUTED FOR ANN AND FDS CASES, FROM THE MONTHLY GRIDDED DATA FOR AUGUST AND SEPTEMBER 2017

	August ANN	August FDS	September ANN	September FDS	October ANN	October FDS	November ANN	November FDS
Bias [m/s]	0.14	0.17	0.04	-0.02	0.00	0.03	-0.08	-0.15
RMSD [m/s]	0.55	0.72	0.65	0.65	0.50	0.68	0.56	0.72
Correl. Coef.	0.96	0.93	0.92	0.92	0.96	0.91	0.94	0.90

The ANN RMSD improves by 15% compared to the FDS case. Improvements similar to those observed for all winds are obtained for winds below 12 m/s, as these represent the majority of the population. For winds above 12 m/s, the errors are higher in both cases, and even the ANN approach is no longer unbiased, but there is still a ~17% improvement in the bias, and a 6% improvement in the RMSD.

Figs. 6 and 7 show a comparison between monthly gridded WW3 wind speeds, CYGNSS ANN wind speeds, and FDS wind speeds. The grids are 0.5° latitudes x 0.5° longitudes in size, and Figs 6 and 7 show maps respectively for August and September 2017. For August 2017 (see Fig. 6) the maps of ANN wind speeds agree well with WW3, and the agreement is globally better than that achieved with FDS winds. The bias between WW3 and FDS winds shows instances of strongly positive biases, which are much attenuated in the case of ANN. The improvement in the bias map for the ANN case compared to the FDS case is also clearly visible for September 2017, especially off the eastern and western coasts of South America. A very good agreement is also observed in Fig. 8, between ANN and WW3 winds for October and November 2017. The bias patterns in the ANN case appear quite consistent between September and November 2017, while they are overall stronger in the month of August 2017. Stronger biases can be seen around the coastal regions for all months, most likely due to more complex ocean and wind processes, different from the open ocean, as well as possible land contamination in the CYGNSS data. Overall monthly statistics of bias, RMSD and correlation coefficient are computed from the gridded data, separately for the two months, and reported in Table IV. The values of bias and RMSD are low

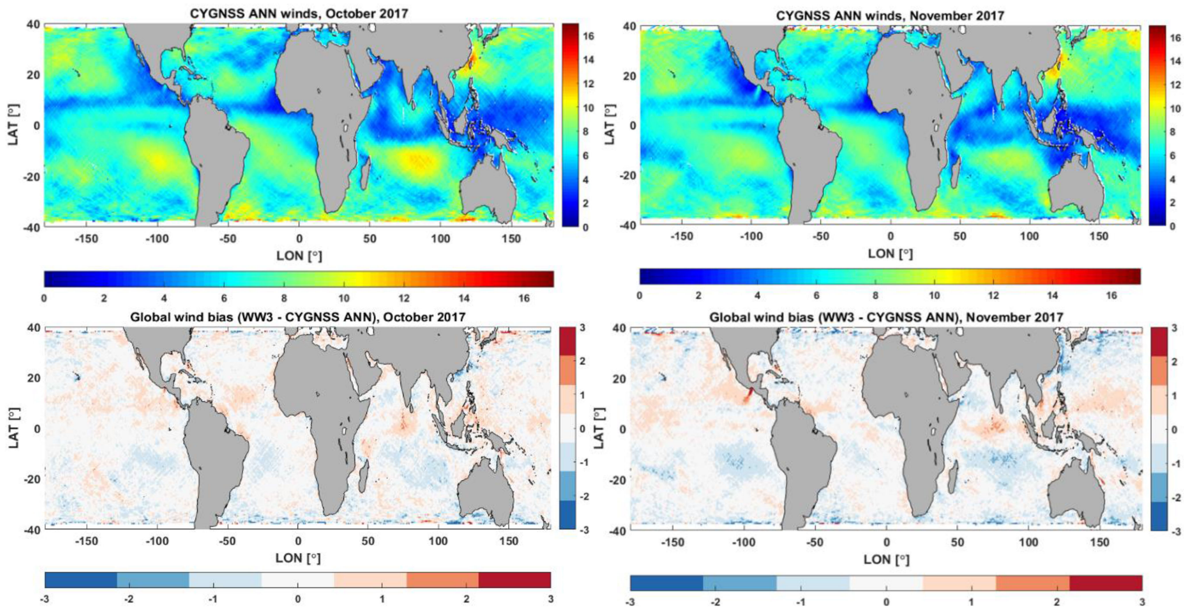

Fig. 8. Illustration of global monthly gridded maps for October (left) and November (right) 2017. The top row shows CYGNSS ANN winds, the bottom row shows the global monthly bias with respect to WW3 winds.

for both FDS and ANN and for all months, but ANN typically outperforms the baseline approach, especially for what concerns the RMSD which improves by more than 20%.

V. Conclusion

Feed-forward ANNs, commonly employed in remote sensing and Earth Observation, were applied to estimate wind speeds from GNSS-R CYGNSS data. The network requires five input parameters, and the optimal number of layers and neurons were chosen based on simple error and correlation metrics. The ANN approach was followed by the application of a CDF matching technique, similar to what is done conventionally in scatterometry. The resulting ANN winds agreed very well with the wind matchups from the WW3 model. The error statistics provided by the ANN are improved with respect to the baseline error, and over the full dynamic range of wind speeds. In particular, the ANN provided unbiased wind estimates over a dynamic range of wind speeds up to 32 m/s, with a RMSD of 1.51 m/s, which is the lowest seen so far in literature for wind retrieval from CYGNSS data. Global wind maps from August to November 2017 agree with WW3 winds almost everywhere. The comparison with baseline FDS winds which represent the official L2 CYGNSS wind product highlights improved winds estimations using the ANN methodology, demonstrating that ANNs were a useful and possibly better method for wind speed estimations than those routinely adopted for CYGNSS at present. The approach presented could be in principle applied to the entire CYGNSS dataset to produce an enhanced wind speed product from CYGNSS. The ANN methodology presented here also suffers from some limitations, such as the difficulty to estimate unusual occurrences of very low or very high wind speed (such as those in tropical cyclones) and the need for a large training set to obtain accurate retrievals over a time frame of several months or years. The tendency of ANN to overestimate the lower values and underestimate the higher ones has been already pointed out in past works (e.g. [17]). It can be explained by considering that the training is based on an iterative minimization of the error variance on the entire training set, in which highest and lowest values are in general poorly represented due to their low occurrence. Moreover, the reduced sensitivity of the CYGNSS data to the highest values of wind speed could also contribute to the high wind underestimations.

Further refinements of the ANN architecture and of the sampling strategy for generating the training set could allow reducing the amount of data required for training and therefore enabling the extension of the analysis to longer time periods. In this respect, it should be noticed that the ANN training is the only time demanding step in setting up the retrieval algorithm, while applying a trained ANN to a dataset other than the training set can be achieved in near real time. Ongoing work will concentrate on further refinement of the ANNs, using a larger dataset rather than only four months of data to train and test the network, and providing further inputs to the ANN—such as GPS satellite ID, CYGNSS satellite ID, and CYGNSS antenna ID—to possibly mitigate some of the calibration problems highlighted so far in CYGNSS [28], [38]. The inclusion of wave information sufficiently decorrelated with wind speed as further input to the network could also contribute to an additional improvement of the final retrieved winds. The performance of the network will be also be tested on a temporally blind dataset. Using a dataset that is completely independent temporally from the data that has been seen by the neural network when training will further validate the results. As in the case of scatterometry [17], [18], an ANN approach could also be implemented and tested to retrieve winds in non-ordinary conditions, such as over tropical storms or cyclones. The CYGNSS wind speed estimations over such storms currently suffer from large noise and errors in the retrieval, and ANNs or more in general machine learning approaches could be attempted to improve the retrievals in these special weather circumstances.

Acknowledgment

The authors would like to thank the reviewers for their in-depth reviews and comments which have helped to improve this article.

References

[1] C. Ruf, S. Gleason, and D. S. McKague, "Assessment of CYGNSS Wind speed retrieval uncertainty," *IEEE J. Sel. Top. Appl. Earth Observ. Remote Sens.*, vol. 12, no. 1, pp. 87–97, Jan. 2019.

[2] B. Annane, B. McNoldy, S. Leidner, R. Hoffman, R. Atlas, and S. Majumdar, "A study of the HWRF analysis and forecast impact of realistically simulated CYGNSS observations assimilated as scalar wind speeds and as VAM wind vectors," *Monthly Weather Rev.*, vol. 146, no. 7, pp. 26–36, 2018, doi: 10.1175/MWR-D-17-0240.1.

[3] S. Leidner, B. Annane, B. McNoldy, R. Hoffman, and R. Atlas, "Variational analysis of simulated ocean surface winds from the cyclone global navigation satellite system (CYGNSS) and evaluation using a regional OSSE," *J. Atmos. Ocean. Technol.*, vol. 35, no. 8, pp. 1571–1584, 2018, doi: 10.1175/JTECH-D-17-0136.1.

[4] Z. Cui, Z. Pu, V. Tallapragada, R. Atlas, and C. S. Ruf, "Impact of CYGNSS ocean surface wind speeds on numerical simulations of hurricanes harvey and irma (2017)," *Geophys. Res. Ltrs.*, vol. 46, no. 5, pp. 2984–2992, 2019, doi: 10.1029/2019GL082236.

[5] D. Mayers, and C. S. Ruf, "Tropical cyclone center fix using CYGNSS winds," *J. Appl. Meteorolog. Climatol.*, vol. 58, no. 9, pp. 1993–2003, 2019, doi: 10.1175/JAMC-D-19-0054.1.

[6] M. P. Clarizia, and C. S. Ruf, "Wind speed retrieval algorithm for the cyclone global navigation satellite system (CYGNSS) mission," *IEEE Trans Geosci. Remote Sens.*, vol. 54, no. 8, pp. 4419–4432, Aug. 2016.

[7] C. S. Ruf *et al.*, "New ocean winds satellite mission to probe hurricanes and tropical convection," *Bull. Amer. Meteorolog. Soc.*, vol. 97, no. 3, pp. 385–395, Mar. 2016, doi:10.1175/BAMS-D-14-00218.1.

[8] C. Ruf and R. Balasubramaniam, "Development of the CYGNSS geophysical model function for wind speed," *IEEE J. Sel. Top. Appl. Earth Observ. Remote Sens.*, vol. 12, no. 1, pp. 66–77, Jan. 2019.

[9] C. S. Ruf *et al.*, "In-orbit performance of the constellation of CYGNSS hurricane satellites," *Bull. Amer. Meteorolog. Soc.*, vol. 100, no. 10, pp. 1–46, 2019, doi: 10.1175/BAMS-D-18-0337.1.

[10] S. Gleason, C. S. Ruf, A. O'Brien, and D. S. McKague, "The CYGNSS level 1 calibration algorithm and error analysis based on on-orbit measurements," *IEEE J. Sel. Top. Appl. Earth Obsserv. Remote Sens.*, vol. 12, no. 1, pp. 37–49, Jan. 2019.

[11] K. Hornik, "Multilayer feed forward network are universal approximators," *Neural Netw.*, vol. 2, no. 5, pp. 359–366, 1989.

[12] A. Linden, and J. Kinderman, "Inversion of multi-layer nets," in *Proc. Int. Joint Conf. Neural Netw.*, Washington, DC, USA, 1989, vol. 2, pp. 425–430.

[13] F. Del Frate, P. Ferrazzoli, and G. Schiavon, "Retrieving soil moisture and agricultural variables by microwave radiometry using neural networks," *Remote Sens. Environ.*, vol. 84, no. 2, pp. 174—183, 2003, doi: 10.1016/S0034-4257(02)00105-0.

[14] A. Elshorbagy, and K. Parasuraman, "On the relevance of using artificial neural networks for estimating soil moisture content," *J. Hydrol.*, vol. 362, pp. 1–18, Nov. 2008.

[15] E. Santi, "Neural Networks applications for the remote sensing of hydrological parameters," in *Artificial Neural Networks-Models and Applications Book*, London, U.K.: InTech Open, 2016.

[16] E. Santi, S. Paloscia, S. Pettinato, and G. Fontanelli, "Application of artificial neural networks for the soil moisture retrieval from active and passive microwave spaceborne sensors," *Int. J. Appl. Earth Observ. Geoinf.*, vol. 48, pp. 61–73, 2016.

[17] B. W. Stiles, and R. S. Dunbar, "A neural network technique for improving the accuracy of scatterometer winds in rainy conditions," *IEEE Trans. Geosci. Remote Sens.*, vol. 48, no. 8, pp. 3114–3122, Aug. 2010.

[18] B. W. Stiles *et al.*, "Optimized tropical cyclone winds from quiksCAT: A neural network approach," *IEEE Trans. Geosci. Remote Sens.*, vol. 52, no. 11, pp. 7418–7434, Nov. 2014.

[19] K. Kasantikul, D. Yang, and Q. Wang, "Coastal ocean wind speed estimation based GNSS-Reflectometry of BeiDou GEO satellite," in *Proc.OCEANS-MTS/IEEE Kobe Techno-Oceans*, May 2018, pp. 1–4.

[20] K. Kasantikul, D. Yang, Q. Wang, and A. Lwin, "A novel wind speed estimation based on the integration of an artificial neural network and a particle filter using BeiDou GEO reflectometry," *Sensors*, vol. 18, no. 10, pp. 1–16, 2018

[21] F. Wang, D. Yang, B. Zhang, and W. Li, "Waveform-based spaceborne GNSS-R wind speed observation: Demonstration and analysis using UK TechDemoSat-1 data," *Adv. Space Res.*, vol. 61, no. 6, pp. 1573–1587, 2018.

[22] Y. Liu, I. Collett and Y. J. Morton, "Application of neural network to GNSS-R wind speed retrieval," *IEEE Trans. Geosci. Remote Sens.*, vol. 57, no. 12, pp. 9756–9766, Dec. 2019.

[23] Q. Yan, W. Huang, and C. Moloney, "Neural networks based sea ice detection and concentration retrieval from GNSS-R delay-Doppler maps," *IEEE J. Sel. Top. Appl. Earth Observ. Remote Sens.*, vol. 10, no. 8, pp. 3789–3798, Aug. 2017.

[24] Q. Yan, and W. Huang, "Sea ice sensing from GNSS-R data using convolutional neural networks," *IEEE Geosci. Remote Sens. Lett.*, vol. 15, no. 10, pp. 1510–1514, Oct. 2018.

[25] P. C. Deka, and R. Prahlada, "Discrete wavelet neural network approach in significant wave height forecasting for multistep lead time," *Ocean Eng.*, vol. 43, pp. 32–42, 2012.

[26] K. L. Hsu, X. Gao, S. Sorooshian, and H. V. Gupta, "Precipitation estimation from remotely sensed information using artificial neural networks," *J. Appl. Meteorol.*, vol. 36, no. 9, pp. 1176–1190, 1997.

[27] A. Wu, W. W. Hsieh, and B. Tang, "Neural network forecasts of the tropical Pacific sea surface temperatures," *Neural Netw.*, vol. 19, no. 2, pp. 145–154, 2006.

[28] M. P. Clarizia, and C. S. Ruf, "Statistical derivation of wind speed from CYGNSS Data," *IEEE Trans. Geosci. Remote Sens.*, 2020.

[29] F. J. Wentz, and D. K. Smith, "A model function for the ocean-normalized radar cross section at 14 GHz derived from NSCAT observations," *J. GeoPhys. Res., Oceans*, vol. 104, no. C5, pp. 11499–11514, 1999. [Online]. Available: http://dx.doi.org/10.1029/98JC02148

[30] E. Andersson, A. Persson, and I. Tsonevsky, *User Guide to ECMWF Forecast Products.* vol. 2.1, Reading, U.K.: ECMWF, 2015.

[31] S. Nissen, "Implementation of a fast artificial neural network library (fann)," Dept. Comput. Sci. Univ. Copenhagen, Rep., vol. 31, p. 29, 2003.

[32] H. B. Demuth, M. H. Beale, O. De Jess, and M. T. Hagan, *Neural Network Design*, Stillwater, OK, USA: Martin Hagan, ch. 22, pp. 21.1–21.30.

[33] D. Svozil, V. Kvasnicka, and J. Pospichal, "Introduction to multi-layer feed-forward neural networks," *Chemometrics Intell. Lab. Syst.*, vol. 39, no. 1, pp. 43–62, 1997.

[34] S. Agatonovic-Kustrin and R. Beresford, "Basic concepts of artificial neural network (ANN) modeling and its application in pharmaceutical research," *J. Pharmaceutical Biomed. Anal.*, vol. 22, no. 5, pp. 717–727, 2000.

[35] L. Prechelt, "Early stopping-but when?," in *Neural Netw., Tricks Trade*, pp. 55–69, 1998.

[36] F. Saïd, S. Soisuvarn, Z. Jelenak and P. S. Chang, "Performance assessment of simulated CYGNSS measurements in the tropical cyclone environment," *IEEE J. Sel. Top. Appl. Earth Observ. Remote Sens.*, vol. 9, no. 10, pp. 4709–4719, Oct. 2016.

[37] M. P. Clarizia, V. Zavorotny, and C. Ruf, "CYGNSS algorithm theoretical basis document level 2 wind speed retrieval," *CYGNSS Project Document 148-0138*, vol. Rev 5, Aug. 2018.

[38] T. Wang, C. S. Ruf, B. Block, D. S. McKague, and S. Gleason, "Design and performance of a GPS constellation power monitor system for improved CYGNSS L1B calibration," *IEEE J. Sel. Top. Appl. Earth Observ. Remote Sens.*, vol. 12, no. 1, pp. 26–36, Jan. 2019.

[39] M. Asgarimehr, I. Zhelavskaya, G. Foti, S. Reich and J. Wickert, "A GNSS-R geophysical model function: Machine learning for wind speed retrievals," *IEEE Geosci. Remote Sens. Lett.*, 2019.

[40] H. L. Tolman, User manual and system documentation of WAVEWATCH III version 3.14., 2009 NOAA/NWS/NCEP Tech. Note 276, 220. [Online]. Available: http://nopp.ncep.noaa.gov/mmab/papers/tn276/MMAB_276.pdf

Jennifer Reynolds received the bachelor's degree in environmental science from the University of Exeter, Exeter, U.K., in 2017 and the master's degree in space and exploration systems from the University of Leicester, Leicester, U.K., in 2018.

Her bachelor's thesis was on using machine learning techniques to estimate the number of dust devil tracks in the Argyre and Hellas Planitia regions of Mars. Since 2018, she has been a Global Navigation Satelite System (GNSS) Reflectometry Engineer with Deimos Space, Harwell, Oxford, U.K. Her work includes, GNSS-Reflectometry, retrieval algorithms, data analysis and machine learning.

Maria Paola Clarizia (Senior Member, IEEE) received the master's degree in telecommunications engineering from the University of Sannio, Benevento, Italy, in 2007, and the Ph.D. degree in ocean remote sensing using GNSS-Reflectometry (GNSS-R) from the University of Southampton, Southampton, U.K., in 2012.

She has more than 10 years of experience in remote sensing, with a focus on GNSS-R, working in both academia and private industry. She has been a Research Engineer with Starlab, Barcelona, Spain, a Research Scientist with the National Oceanography Centre, Southampton, U.K., and a Postdoctoral Research Fellow with the University of Michigan, Ann Arbor, MI, USA, and with the University of Southampton, Southampton, U.K., working on the National Aeronautics and Space Administration (NASA) Cyclone Global Navigation Satellite System (CYGNSS) Mission for ocean and land applications. She is currently a GNSS-R Technical Manager with Deimos Space, Harwell Oxford, U.K., and a member of the CYGNSS Science Team. Her current research interests include GNSS-Reflectometry, altimetry and scatterometry, electromagnetic scattering models, retrieval algorithms, data analysis, and statistical processing.

Emanuele Santi (Member, IEEE) received the M.S. degree in electronic engineering from the University of Florence, Florence, Italy, in 1997, and the Ph.D. degree in earth's remote sensing techniques from the University of Basilicata, Potenza, Italy, in 2005.

Since 1998, he has been a researcher, with the Microwave Remote Sensing Group at Institute of Applied Physics of the National Research Council. He was and is currently involved in many national and international projects (ASI, EC, ESA, JAXA), acting as Team Leader, WP Leader or co-I. He is and author or co-author of 138 papers, published on ISI journals and books and conference proceedings. His research interests include development and validation of models and statistical inversion algorithms for estimating the geophysical parameters of soil, sea, snow and vegetation from microwave emission and scattering.

Dr. Santi is a Member of the Institute of Electric and Electronic Engineers (IEEE) and of the "Centro di Telerilevamento a Microonde (Microwave Remote Sensing Center)". He is also Conference Chair of the SPIE Europe Remote Sensing. In 2018, he was the recipient of IEEE GRSS J-STARS Prize Paper Award for the best paper published on the J-STARS journal in 2017.